Highlights

Experimental Testing and Magnetic Resonance Imaging to Determine Mechanical Parameters of the Intervertebral Disc: Testing Techniques and Results

Claudia D'Agostino,Rea Metaj

- Properties of the intervertebral disc
- MRI protocols
- Mechanical testing protocols
- Empirical correlations between MRI and biomechanical data

Experimental Testing and Magnetic Resonance Imaging to Determine Mechanical Parameters of the Intervertebral Disc: Testing Techniques and Results

Claudia D'Agostino[a], Rea Metaj[a]

[a]*Politecnico di Torino, corso Duca degli Abruzzi, 24, Torino, 10129 TO, Italy*

ARTICLE INFO

Keywords:
intervertebral disc
mechanical testing
magnetic resonance imaging
mechanical parameters
disc degeneration

ABSTRACT

The intervertebral disc is an element of the human spine that has been extensively studied through different approaches to provide an understanding of its biomechanics and functions, with the main objective of proposing treatments and measures regarding several pathologies that concern it. The aim of this report is to analyze mechanical testing and magnetic resonance imaging of the disc, while presenting the correlations between the results of the two methods. This vertebral component itself may be considered as part of a spinal unit, as an individual sample, or divided in its constituents, the annulus fibrosus and the nucleus pulpous. Conducted experiments, in vivo or ex vivo, asses the spine component though mainly compressive loading protocols, or alternatively through traction and bending. Magnetic resonance mapping is predominantly performed to classify the disc's grade of degeneration. This overview has been constructed around a central article of choice, that better represents the findings on the matter, while distinguishing similarities and divergences with other considered articles. The dependency of material properties of the intervertebral disc and its imaging characteristics is greatly observed; however, quantification of associative data and derivation of empirical formulae is rarely computed.

1. Introduction

1.1. Intervertebral discs

Intervertebral discs (IVDs) are fibrocartilaginous elements of the intervertebral junction, interposed through adjacent vertebrae of the spine [5, 27]. They allow the binding of the vertebrae, while conferring mobility and support to the column, acting as a shock absorber and contrasting traction, compression, torsion, and shear solicitations deriving from movements of the body. Each disc is composed of three portions: nucleus pulpous (NP), annulus fibrosus (AF) and cartilaginous endplates [25].

The NP is an amorphous gel-type structure that occupies 40-50% of the complete IVD volume, consisting in collagen type II, proteoglycans, and water. Its high-water content, which may amount up to 88% components, generates swelling properties and a hydrostatic pressure in the nucleus, permitting it to exercise a compressive force, which varies with loading [29, 46, 14].

The AF is a fibrillar structure composed of collagen type I organized in concentric alternating layers surrounding the NP, denoted as lamellae, whose thickness decreases outwardly. The three-dimensional architecture of this element varies as a function of vertebral level and intradiscal region, with a mean inclination of the bands of 60° with respect to spinal axis. Compressive stress from the NP is transferred to the AF lamellae, whose geometry offers support during torsion, flexion, and extension [27, 14].

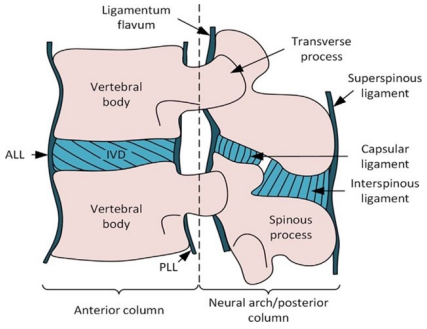

Figure 1: [54] Graphical representation of a motion segment in a sagittal view, denoting intravertebral discs, adjacent vertebral bodies, ligaments and vertebral processes.

1.2. Magnetic resonance imaging and biomechanical properties of intervertebral discs

The three-dimensional organization of the IVD and its components is responsible for the structure's mechanical properties [65]. IVD behavior can be described as non-linear, anisotropic, and viscoelastic, representing biphasic material characteristics, which is conferred by its macromolecules and water content [14, 67].

Magnetic resonance imaging (MRI) functions through proton interaction with a magnetic field, allowing the visualization and analysis of tissues high in positive ions. The high proton density of the IVD environment allows for accurate MRI evaluation of the matrix composition.

Such imaging technique may be used to correlate biomechanical properties to its MR parameters, since both are dependent from IVD components and architecture [9].

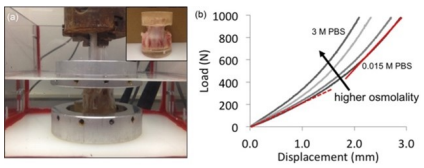

Figure 2: [11] (a) Mechanical testing of a spine motion segment. (b) Force-displacement curve and hydration dependency.

The NP and the AF are the main elements of the disc that are studied for correspondences between imaging and experiments, excluding the endplate portion whose degeneration processes are reportedly not of biomechanical origin [60].

2. Mechanical testing

Mechanical testing is performed to characterize IVD tissue, to understand its functions as a sole element and in relation to others, and to find prosthetic materials when partial or complete discectomies are performed [41].

The findings of loads on the lumbar segment of the human spine, examined by Nachemson, have served as pillars for following studies. Methods used to compute intradiscal pressure and its relations to different inclinations of the column are up to now contemplated as valid and taken into consideration when studying this matter [51].

The type of experiments executed to assess IVD properties is based on the function of the element in exam. AF is evaluated in uniaxial and biaxial tension, compression, shear, and torsion, due to its lamellar configuration and general anisotropy; NP is studied in compression, shear, and torsion, as a generally isotropic component, which confers stability and flexibility to the spine [52]. The disc can be tested as a single sample, or combined with its endplates and adjacent vertebrae, as to consider the effects of other surrounding structures, as musculature, bones etc. Methods that test IVDs or spine units include axial compression, bending and rotation [54].

Tissue engineering of the IVD components adopts different models to represent the AF and NP separately, or the entire disc, while computing material properties. Reported parameters are comprised of intradiscal pressures, ranges of motion, strains, stiffnesses, tensile moduli, Poisson's ratios, aggregate moduli, hydraulic permeabilities, shear moduli etc. [41]. Stress-displacement calculations limit their definitions of the IVD to elastic and viscoelastic definitions, as to simplify results and to better correlate to possible prosthetic materials [52].

3. Magnetic resonance imaging

3.1. Imaging technique

Magnetic resonance imaging (MRI) is a non-invasive imaging method used to visualize internal structures within the body. It functions through emissions of non-ionizing, radio frequency radiation while generating a magnetic field. The magnetic field aligns nuclei of atoms, generally marking

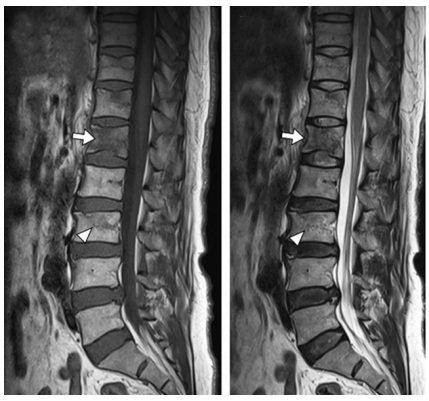

Figure 3: [37] (A) Sagittal T1-weighted MRI of the lumbar spine. (B) Sagittal T2-weighted MRI of the lumbar spine.

Hydrogen nuclids, which are targeted by the radiation. The mapping is achieved by detecting the energy released after the interaction and during the return to the original state, a process denoted as relaxation [36].

During MRI, many temporal parameters are measured, such as the rate of return of net magnetization to equilibrium (T1), the rate of loss of transverse magnetization (T2), short repetition time (TR), echo of signal recovery time (TE), spin density (SD) etc. These characteristics can be quantified, and their values offer information regarding the properties of the tissue they individuate, by distinguishing alterations in relaxation times [36].

3.2. Magnetic resonance imaging of the spine and intervertebral discs

MRI has become the golden standard for imaging of the vertebral column and its components, as it allows to accurately distinguish soft tissues and individual elements. The technique offers remarkable details of the morphology of IVDs, making it often preferred to diagnose disc pathologies and evaluate degeneration [37]. Considering that the AF is primarily composed of collagen fibers, elements also present in the NP, MRI is one of the most adequate methods to properly visualize these structures and their anatomy [83] .

3.3. Intervertebral disc degeneration

IVD degeneration is an irreversible cell-mediated process that may be defined as a structural degradation. This development influences and alters the discs' anatomy, metabolism, histological composition, function and therefore its mechanical parameters. Furthermore, it may be disruptive of other adjacent structures [5].

The determination of the disc's integrity is possible through imaging evaluations. These exams assign a grade based on qualitative scales that define degenerative advancement. Several scales exist, which grade IVDs by evaluation of imaging parameters and disc anatomy visualization, with the Thompson and the Pfirrmann score being the most frequently utilized.

The Thompson scale grades IVDs based on their gross morphology, attributing five categories from I-V, depending on degeneration progress [34]. The scheme is often adopted for analysis of MR images and disc dissections.

The Pfirrmann score classifies IVDs in five categories from group I (healthy discs) to group V (severely degenerated discs) [58]. This technique is preferred when visualizing MR images. Some modifications of this system have been proposed, like an increase of the score from 5 to 8, or a quantitative system less prone to error, however, the original grading system remains the most used [63, 22].

3.4. T1 and T2 relaxation times

The most common MRI sequences are T1-weighted and T2-weighted scans. T1-weighted images are produced by using short TE and TR times, while T2-weighted images are produced by using longer TE and TR times.

In T1-weighted images, fat is represented with the lightest tones as it is characterized by the shortest net relaxation times, thus naming the results fat images. This method is preferred when analyzing the anatomy of a component, as it provides highly detailed visualizations with high spatial resolution.

In T2-weighted images, water is represented with the lightest tones as it is characterized by the longest transverse relaxation times, thus naming the results water images. The technique is generally used when analyzing abnormal tissues, such as in inflammatory changes or tumors [36].

3.5. T2-weighted images and intervertebral discs

Both types of pulse sequencies are executed to allow for individualization of different tissues. However, when investigating highly hydrated elements as IVDs, T2-weighted images are favored as they are also correlated to tissue anisotropy, collagen concentration and age of the subject [43]. T2 relaxation times are usually calculated on a pixel-by-pixel basis, by curve fitting the relationship between signal intensity (SI) and TE: $SI = SI_0 exp\frac{-TE}{T2}$, with programs such as MATLAB [81].

T2-weighted imaging may be conducted in sagittal, axial, and coronal directions. Axial acquisition appears slightly more sensitive to disc degeneration individualization [77]. Nonetheless, the necessity to determine the center of the disc requires a further T1 scan. Therefore, sagittal T2 images are greatly preferred.

Despite T2-weighted sequences being the standard for disc visualization, other less used methods can offer more precise results that may correlate to mechanical properties.

3.6. T1rho magnetic resonance imaging

T1rho, referring to a "ro"tating frame, is an MRI sequence developed primarily for use in musculoskeletal imaging, integrating elements of both T1 and T2 mapping. The parameter is superior to T2 when determining proteoglycan content and early stages of degeneration [33, 50, 61]. Consequently, these scans are performed for investigating healthy to moderately degenerate discs, that tend to have less distinctions than more degenerate ones in axial T2-weighted imaging.

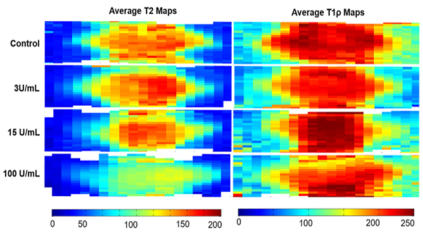

Figure 4: [23] Population average T2 and T1r maps.

3.7. Diffusion tensor imaging, apparent diffusion coefficient and fractional anisotropy

Diffusion tensor imaging (DTI) or diffusion-weighted imaging (DWI), comprises a group of techniques where calculated eigenvalues and eigenvectors are used to create images reflecting various diffusion properties of a tissue. The technique is utilized to derive formulas regarding IVD stiffness [70].

The apparent diffusion coefficient (ADC) or its trace (TrD), an average of the eigenvalues, is a DTI parameter often used to determine correlations [50]. It has been proven to not be a meaningful specification when considered individually, as it is less correlated to age and degeneration than other MRI outcomes [56].

Fractional anisotropy (FA) is an index of the material's anisotropic properties which can measure microstructural characteristics of the NP and single collagen morphology, making it suitable to detect early degeneration [70, 69].

3.8. Echo times

The most used sequence, when using specific parameters like T1rho, T2*, or SPACE sequencies, is fast spin-echo (FSE), alternatively turbo-spin echo (TSE) [40]. Ultrashort time echo (UTE) sequencies, particularly FLUTE sequencies, are adequate for visualizing other spine components, including longitudinal, ligamentum flavum, and the CEP, which cannot be mapped through traditional MRI methods [1, 24].

Gradient echo techniques allow for the measure of T2 values in a 1-2 ms range, which enables AF imaging. Nonetheless, the method is inferior to other echo times regarding spatial resolution, tissue visualization, slice thickness and bandwidth [8].

Simple spin-echo sequencies are appropriate when calculating simple T1 or T2 relaxation times to create morphological images used for Pfirrmann or Thompson's grading, but not in the acquisition of quantitative data [85].

3.9. Other magnetic resonance imaging techniques

T2* is a time constant obtained by gradient echo determined in the presence of local magnetic field inhomogeneities, and it is shorter than T2 singularly. The parameter is related to GAG content, particularly in the NP and inner

AF, and residual stresses and exercised strains [21]. The technique presents advantages with respect to T2 scans in detection of early changes in the AF and disc mapping [44, 79], while being inferior to specific methods as DVC or DTI [12, 24].

Magnetization Transfer Imaging (MTI) is a technique that applies radiofrequency energy exclusively to the bound pool, used complementary to DTI [50, 59]. It is quantified through the magnetization transfer ratio and contrast (MTR and MTC), acquired by digital subtraction of two sets of images.

The Otsu method is an image binarization technique used on MRI scans to accurately determine perimeters and the TOtsu threshold, a parameter linked to disc degeneration grade and stiffness. Its results are employed as supplementary information [42].

Gadolinium enhanced MRI is a contrast procedure performed on cartilage that can be used to correlate material injection to GAG content [75, 74].

Sampling Perfection with Application optimized Contrast (SPACE) sequences are three-dimensional TSE imaging techniques that create high spatial resolution datasets. This type of imaging is advantageous when reconstructing volumes with less sensitivity to susceptibility, flow, and chemical shift artifacts [40].

MR Spectroscopy (MRS) is a nuclear magnetic resonance method used to measure water and GAG content of tissues. Its results can be easily correlated to other MRI parameters, however, are seldom used when relating mechanical properties [86].

Digital Volume Correlation (DVC) is an MRI manipulation executed to obtain displacement and strain results. Its accuracy rivals experimental testing, with an error of 56 µm and 3000 microstrains [71, 72]. Fat suppression is commonly used in MRI to suppress the signal from adipose tissue or detect adipose tissue, however, its use's results on disc imaging are negligible [40].

4. Materials and methods

4.1. Chosen article

Articles that analyze the human spine and IVDs conduct experiments and evaluations to provide an understanding of the biomechanics of these elements. They opt to find correlations between mechanical, histological, behavioral, and imaging parameters, as to provide for solutions and treatments for different pathologies of the vertebral column [28].

The chosen article [6] describes the approach to the problem of low back pain, an illness that affects a considerable percentage of the population in developed countries [38], through quantification of MRI and biomechanical properties, in relation to the degeneration levels of IVDs.

Briefly, the paper describes axial and dynamic loading of dissected AF and NP, MR mapping and computation of its features, histological assessment for different degeneration grades, correlation, and linear regression analysis of the experiment's results.

4.2. Specimens and experimental groups

Ten spine units belonging to the lumbar and sacral portion of the column of human cadavers were obtained postmortem for experimentation. Fifty discs were excised, and AF and NP sections were obtained through biopsy punches.

The most investigated portions of the spine are the lumbar, sacral, and cervical levels [18, 39]. The choice derives from the pathologies in exam, which mainly include low-back pain and herniations, the high quantity of samples acquirable from these regions, and the susceptibility of the zones to physiological loading and movements [31, 68, 35].

Ideally, in vivo human experiments should be used to characterize IVD [48]. However, due to low subject participation, limited applicable forces, and few non or little invasive techniques executable, ex vivo tests are mainly performed.

In vitro analyses utilize human or animal cadavers, which are preferably harvested near the time of death [50, 13, 55]. The components undergo deep freezing before testing, a procedure that is generally recognized to produce little or no effect to the discs' properties [20].

4.3. Magnetic resonance imaging

The MRI examinations were carried out in a 1.5 Tesla whole-body Siemens' Avanto system, measuring T1, T2, MTR, and ADC for NP and AF in a sagittal orientation.

While the MR systems, the field strength and imaging orientation differ throughout experiments, the measured parameters include mainly T1 and T2 relaxation times, which can be accompanied by MTI and DWI parameters like MTR, ADC and FA [61, 59]. T1rho measurements [23], ADC trace [59] and spin density computations are also observed [81].

The discs were rated using Pfirrmann's grading system [58] based on T2-weighted images, as to link the properties observed through mechanical testing to the disc's degenerative state. It was observed that both T1 and T2 relaxation times decreased in both NP and AF tissues with degeneration. Histological evaluations, often performed in addition to imaging, confirm the gradual alteration of the NP and AF matrix with increasing Pfirrmann grades.

4.4. Regions of interest and geometry

Quantitative MRI (qMRI) parameters were calculated considering two regions of interest (ROIs), manually traced as polygonal shapes to represent both NP and AF regions, omitting endplate tissue, as shown in Figure 5. This division into ROIs allows the evaluation of the characteristics of the AF and NP separately, an approach utilized in many experiments [50]. Nonetheless, this separation can be omitted when considering the disc as a homogenous material [23] or for analysis one single region of interest, NP, or AF [59].

MRI can be used as a tool to assess the disc's geometry, an important characteristic when generating evaluation models. The IVD's height, area or volume can be accurately

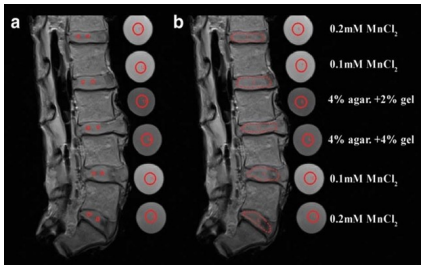

Figure 5: [6] Regions of interest traced (a) separately for anulus fibrosus and nucleus pulposus, (b) for the entire disc.

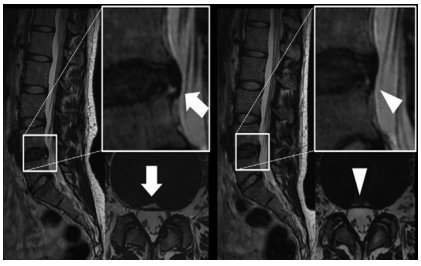

Figure 6: [19] Disc changes observed through in vivo MRI before (left) and after (right) 30 minutes of traction.

measured, with fewer errors than the traditional anterior or posterior height techniques. Different protocols have been developed, including altitude evaluation with dependence of area and age, centroid methods etc. [64**?**]. Complete geometry can be obtained through single or double scans, eliminating the necessity to perform differently orientated acquisitions.

4.5. Spine and intervertebral disc magnetic resonance imaging ex vivo

The imaging may be acquired before and after the experimental test, for a consequent qualitative or quantitative comparison of MR and biomechanical parameters [50].

To allow for adequate mapping and imaging quantification, mechanical testing may be executed while in the MR scanner. Specific loading frames are constructed of non-magnetic materials, as to not disturb the magnetic acquisition [57].

Field strength of the imaging technique is commonly found to be of 1,5 T and 3 T, as most clinical scanners have the characteristic pre-programmed. Investigations between different values of the magnetic field have found its variations to be negligible [15].

4.6. Spine magnetic resonance imaging in vivo

MRI is clinically performed with the subject in a supine position, with repercussions of spine flexion and absence of load on the column. To achieve acquisitions with physiological forces on the spine, specific loading MR-compatible apparatuses are utilized to axially compress the spine, simulating erect position circumstances [66].

Vertically open-configuration MR systems are imaging devices that allow for erect or seated positioning of a subject. Weight-bearing exams of the vertebrae and IVDs can be used for static experiments or kinetic ones, combining load with flexion, extension, and rotational movements. These machines are adequate for physiological conditions; however, their spatial resolution is compromised due to field inhomogeneity of the vertical positioning [78].

4.7. Whole section vs single intervertebral disc

The IVDs are components of the spine that are connected to other structures, such as vertebrae, muscles, ligaments etc. [27]. These elements relate to one another structurally, physiologically, and mechanically, therefore, individual measurements may not be accurate or exhaustive, as not representative of relationships created by the coupling of the constituents [74].

During testing, the IVDs may be analyzed as part of a complete motion segment, consisting in IVDs and adjacent vertebral bodies, or as excised components. Furthermore, the components of the disc, NP, and AF, may be sectioned and studied separately. Mainly, vertebral units or disc originating from the lumbar or cervical portions of the spine are extracted [61, 6, 57].

4.8. Model considerations

The AF of the disc was analyzed in confined compression, whereas both AF and NP were examined in shear. The decisions were based on the known sensitivity to these distinct solicitations of the IVD portions. Testing for grade 5 degenerated specimens were not conducted due to limited samples or deteriorated architecture.

When performing mechanical experimentations, IVD architecture must be considered during the process design. Certain models attempt to model discs as biphasic materials, composed of a solid and a liquid zone [33]. In other tests, the dependence of properties on position and interactions of the lamellar structure of the AF, therefore anisotropy of the element, influences the approach, as single fibers, select portions or complete layers may be examined [26, 4]. Nonetheless, similar accuracy in determination of IVD characteristics are observed [54, 59, 42].

Loading levels are also contemplated, as they have different effects on the disc's features. Disc stiffness and Young's Modulus are strain dependent, while IVD geometry is altered by continuous solicitation [54, 59, 53].

4.9. Experimental enviroment

AF portions were tested in an axial compressive machine, were the porous upper platen allowed for the presence of a saline buffer, while both AF and NP portions were tested through a rheometer in a humidified chamber. A dwelling interval of 30 minutes was executed.

The ex vivo testing setting mimics the physiological environment of the spine components, as to induce little alterations to their properties. Temperature and hydration

are controlled, as it has been proven that they affect creep behavior and stiffness of the discs [45, 11].

To allow for water retainment of the disc, different measures can be taken: water spaying, saline soaked gauze wrapping, humidity chamber testing, saline bath immersion etc. [54]

In vivo testing of the subject is often executed during the same time of day, as it has been observed that disc hydration varies diurnally. Experiments are performed early in the morning, during which the discs present their highest water capacity [3].

4.10. Preconditioning and preload

To ensure full contact with the samples and equilibration, 0,15 or 0,1 N forces were achieved through lowering of the platens of the testing machines.

Preconditioning, performed as cycling loading in different directions, serves to prepare the components and minimize their viscoelastic properties. The tests reduce freezing, thawing and immobility repercussions. Three cycles in three principal directions may be sufficient, however many studies put forth a few thousands [30].

Preloading conditions the disc's properties, as its amplitude affects flexibility and stiffness of the element [31]. It is generally performed to achieve adequate contact of the specimen to the apparatus and serves as a reference for further calculations. Amplitude varies throughout different protocols, with static loads observed of 0,1 N to 50 N or strain ramps [6, 55, 57].

4.11. Ex vivo loading

AF units underwent quasi-static axial compression through a single ramp of 5% strain and more than an hour of equilibration dwell. AF and NP samples were subjected to shear dynamic testing at 10% strain for four frequencies from 0,03-30 Hz.

In vitro loading methods may be executed until complete failure of the component, however, loading that replicates physiological forces is generally performed to achieve diagnostic results. Different experiments include axial traction, axial compression, creep, cyclic loading etc. [54].

Confined compression experiments are often performed, through compression chambers, on spinal units, complete IVDs or sectioned NPs and AFs. They may be executed statically, cyclically, or maintained to observe creep behavior. Static magnitudes vary from 40% of average subject weight to thousands of Newtons, while ramps achieve strains of 5-15% [61, 32, 57].

Traction experiments are less frequently performed than compression ones. The technique is executed on complete spine segments or NP and AF segments. Singular portions of the IVD are tested in classic stress-strain conditions [68].

Other mechanical observations include shear examinations, flexion/extension and bending [54].

4.12. In vivo loading

In vivo loading techniques and amplitudes are limited by the the subject's tolerability and effects that may be produced from the solicitations. Different experiments include axial traction, axial compression, flexion/extension, bending etc. [54].

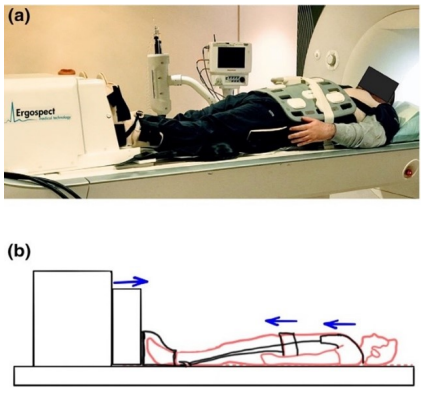

Figure 7: [48](a) Experiment setup. used for mechanical loading during the MRI scan. (b) Schematic of the experimental setup showing how the mechanical load is transferred to the spine.

Traction and compression are achieved through devices generally equipped with harnesses which equally distribute the load, or other non-invasive physiotherapeutically utilized equipment. Magnitudes of the forces applied do not exceed 50% of the subject's weight [66, 19, 80].

Flexion/extension and bending are achieved through postural variations of the subject [73].

4.13. Biomechanical parameters

The AF was fitted to a static biphasic model as to calculate compressive modulus (HA) and hydraulic permeability (k). For the characterization of AF and NP in dynamic conditions, dynamic modulus magnitude (|G*|) and phase angle (δ) were computed through power law exponents, due to their exponential dependence on frequency ($\alpha_{|G*|}$, α_{δ}).

Material properties regarding the complete IVD or its components may be derived through measurements that depend mainly on in or ex vivo loading: continuous displacement calculations, strain field visualization, gauge pressure needle implantations, imaging etc. [61, 13, 30].

By means of load-deformation curves, calculated parameters include neutral zone, range of motion, elastic or compressive stiffness, radial permeability, Poisson's ratio, viscoelasticity, compressive modulus, hydraulic permeability etc. [59, 30]. Using strain fields, internal displacements, Lagrangian strains and tensors may be acquired [82, 16].

Imaging methods are preferred for noninvasive analysis, and the parameters acquired through MRI, CT scans or discography serve as data for element degeneration, mechanical correlations, or observation methods [50, 48, 73, 49].

4.14. Experimental alterations

IVD properties can be also evaluated in relation to its compositional components, mainly water and proteoglycan content. Therefore, in addition to conducting simply mechanical experiments, some studies observe and quantify

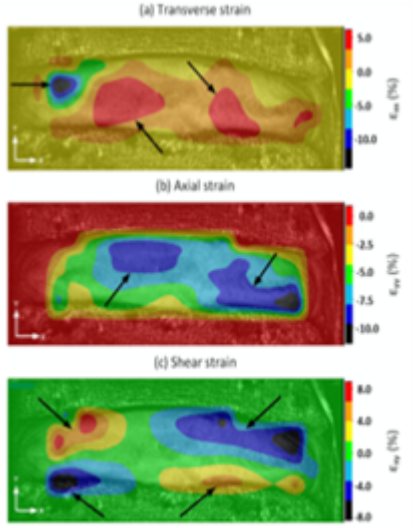

Figure 8: [71] (a) Transverse (exx), (b) axial (eyy), and (c) shear (exy) strain maps shown for a typical sample on the same mid-coronal slice, with strains reported as a percent. Black arrows show both compressive and tensile strain in (a), high axial compressive strains in (b), and peak shear strains close to the endplates in (c).

biomechanical and degeneration alterations at different levels of hydration, by producing suitably overhydrated and underhydrated specimens, or with proteolytic enzyme injections, such as chymopapain or trypsin [50, 61, 59]. It has been generally observed that digestion deteriorates material characteristics and decreases relaxation times, as it significantly alters IVD matrix.

4.15. Strain maps

Mechanical properties of different materials are often acquired through stress-deformation experiments [47]. For acquisition of displacement fields for biomechanical testing of three-dimensional and structurally irregular tissues, such as IVD, MRI can be applied. The mapping technique allows for visualization of the element ex vivo or in vivo, as a non-invasive exam [62].

The image acquisition may be conducted continuously while the loading experiment is executed through MRI-compatible machines [48], allowing for immediate observations. Other procedures opt for data obtainment before and after load application, with one of the frames serving as a reference [62].

Warp fields are successively computed through image processing, which prescribe the movement of pixels, therefore the deformation of the disc [82]. Results of the analysis include stress-deformation graphs, deformation gradient tensors, Lagrangian strain tensors etc. [48, 82]. Degenerate discs tend to have higher axial strains, three-dimensional compressive and shear strains [71].

5. Biomechanical testing, MRI and biochemical assessments

5.1. Biochemical composition

In addition to mechanical testing and MRI, biochemical assessment of the IVD is often performed [50, 59, 49]. Many studies have examined relationships of biochemical components to biomechanics and imaging characteristics separately. Nonetheless, all three techniques offer complementary results, hence providing for the future opportunity of evaluating the disc through correlations between different approaches.

NP and AF tissues are dissected to be studied individually, to determine hydration and molecular composition. Water content is measured through subtraction of wet weight and dry weight, with the former one achieved through heat dehydration. To observe proteoglycan and collagen content, colorimetric assays are performed, using DMMB, hydroxyproline etc. Furthermore, quantification of proteoglycans, collagen and GAGs can be evaluated through digestions of different proteinases, including K proteinase, trypsin, chymopapain etc. [65, 49].

5.2. MRI and biochemical properties

MRI is a technique that may be used to provide information on the morphology of the disc, its molecular composition and structural integrity [74]. The imaging method has been used to assess the content of various components of the disc, as well as observe phenomena such as water transport, molecule movements, element losses etc. Biochemical alterations are responsible for the IVDs degeneration, therefore, it has been suggested that MRI can be used as a tool to verify these variations and detect early degenerative states [50].

Correlations were found between MRI parameters and biochemical composition: T1 relaxation time relates to water, aggrecan and collagen content [74]; T2 relaxation time relates to water, aggrecan and collagen content, and tissue anisotropy [74, 7]; T1rho relates to and can measure proteoglycan, GAG and water content [74, 13]; MTR relates to collagen concentration [6]; ADC relates to molecular mobility, microscopic tissue changes and water transport [74, 6]; MRI spectroscopy can determine proteoglycan and degenerated collagen content [74]; Sodium imaging can measure GAG content and loss [74].

5.3. Biomechanical and biochemical properties

Biochemical exams are executed to quantify the relationship between molecular composition and biomechanical properties. It has been defined that mechanical behavior is determined by the matrix composition and molecular architecture of the IVD, however many observations conclude that molecular structure is dependent on the loads and deformations the disc perceives [74].

Water content is responsible for the viscoelastic, strain-dependent, and compressive behavior of IVD [52]. Hydration varies diurnally, with its express observed during the day due to compression and imbibement during the night. Water retention is related to Sodium Ions, and proteoglycans,

which bind it to the IVD tissue. Hydration in the AF, and especially in the NP, generates osmotic pressure, which in return governs the swelling pressure [74]. Water has been assessed to determine the compressive modulus, therefore compressive behavior [10], however, many studies have found it plays an important role on tensile modulus and tensile characteristics [52].

Proteoglycans and GAGs, principally sulfated-GAGs, can be used as predictors of the mechanical functions of the IVD. They are reported to contrast compressive forces [7], while being generally related to swelling pressure and aggregate modulus [33].

Collagen, as well as proteoglycans, GAGs, and water contents, have been observed to be sensitive to loading [50]. The fibrillar collagen composition is linked to tensile strength [7]. Type I collagen, mainly observed in the AF, offers resistance during tension. Type II collagen binds proteoglycans in a fine meshwork, hence allows for water retainment, which enables the disc to withstand compressive forces [2].

Other elements, such as elastic microfibrils, non-collagenous proteins, elastin etc., have been identified as important components for the discs' structure and biomechanics [74]. Proteins and elastin help for the elastic recoils following large deformations of the IVD [2].

6. Results

Correlations were found for the NP between T2 and shear modulus |G*|, ADC and α_δ, whereas for the AF, T1 was linked to α_δ and permeability k. For the complete IVD dependencies were observed between T1 and $\alpha_{|G*|}$, T1 and α_δ, T1 and k, T2 and compressive hydraulic modulus HA. Graphic representations of the correlations are shown in figure 9.

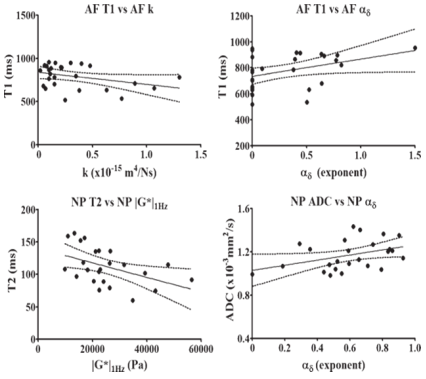

Figure 9: [6] Correlations between MRI (T1, T2 and ADC) and mechanical (permeability, shear modulus and exponential phase angle) parameters.

Different tests examine and calculate mechanical data, including swelling pressure, hydraulic permeability, compressive modulus, dynamic modulus, phase angle, neutral zone modulus, osmotic pressure, opening pressure, gravimetric water content etc., while finding dependency on MR parameters.

The relationship between mechanical properties and MRI data was investigated using linear regression analysis. This approach is used when unable to derive empirical correlations. Linearization and inverse relation, with the latter providing more complex equations, are acquired through different statistical analysis algorithms [33, 17, 84]. Correlations, empirical formulae, and linear regressions are summarized in Table 1.

7. Conclusions

This report reviews different mechanical testing and imaging techniques performed on IVDs. The use of MRI to evaluate mechanical properties is an approach seldom adopted, as the results produce little correlations. Nonetheless, it may be a promising tool in the future.

Parameter	MRI dependance	Formula or linear regression	Reference
Swelling pressure P	T1, T2, T1rho, MTR	P=-862.1+1.237*T1+1.667*T2-2.006*T1rho+1.599*MTR	[50]
	T1rho	-	[55]
Compressive modulus H_A	T1, T2, T1rho, $ADC_{mean}(NP)$	-	[50]
	T2	-	[6]
	T1rho (AF)	-	[50]
	T1, T2, MTR, TrD	$H_{A0} = 3.31 + 0.0006 * T1 + 0.0025 * T2 - 3.05 * TrD + 4.27 * MTR$	[59]
	T2	$T2 = 66.78 + 0.55(\frac{GAG}{NP_{volume}}) - 3.78 * \tau_1 + 6.18 * H_A$	[23]
		$T2 = 87.868 + 5.29 * H_A - 1.92 * \tau_1 + 70 - 49(\frac{Water}{NP_{volume}})$	
Hydraulic permeability k	T1, MTR, ADC (AF)	$k_{AF} = -0.06197 - 0.001272 * T1_{AF} + 1.765 * MTR_{AF} + 1 - 009 * ADC_{AF}$	[6]
	T1, T2, T1rho, MTR, ADC_{mean}	$k = 1.217 - 0.01321 * T1 + 1.207 * T2 - 0.08975 * T1rho - 394.9 * MTR - 122.2ADC_{mean}$	[50]
	T1	-	[50]
	T1, T2, MTR, TrD	$k_0 = -2.14 - 0.0118 * T1 + 0.0066 * T2 + 8.94 * TrD - 2.88 * MTR$	[59]
Dynamic modulus magnitude |G*|	T1, T2, ADC(NP)	$\|G*\|_{1HzNP} = 5189.3 - 322.01 * T2_{NP} + 31 - 130 * T1_{NP} + 26471 * ADC_{NP}$	[6]
	T1,T2	-	[6]
Phase angle δ	T1, ADC	-	[6]
Neutral zone modulus NZM	T1rho	$T1rho = 206.45 + 1.64\frac{GAG}{NP_{volume}} - 23.61(NZM)$	[23]
Osmotic pressure P	T1rho	$P = (\frac{T1rho}{1000})^{1}.6$	[76]
Opening pressure OP	T1rho	-	[13]
Gravimetric water content GWC	SD	$GWC_{NP} = \frac{SD}{-0.74*SD+1.75}$ $GWC_{AF} = \frac{SD+0.14}{1.21}$	[81]

Table 1

References

[1] Conventional and ultrashort time-to-echo magnetic resonance imaging of articular cartilage, meniscus, and intervertebral disk. *Topics in Magnetic Resonance Imaging*, 21:275–289, 10 2010.

[2] Biomechanics of the human intervertebral disc: A review of testing techniques and results. *Journal of the Mechanical Behavior of Biomedical Materials*, 69:420–434, 5 2017.

[3] Malko John A., Hutton William C., Giacometti Andrea R., Kater Gabrielle, Greenfield Paula, Boden Scott D., and Silcox D. Hal. Do diurnal changes in loading affect the interpretation of mri scans of the lumbar spine? *SPINE*, 1996.

[4] Clayton Adam, Philippe Rouch, and Wafa Skalli. Inter-lamellar shear resistance confers compressive stiffness in the intervertebral disc: An image-based modelling study on the bovine caudal disc. *Journal of Biomechanics*, 48:4303–4308, 12 2015.

[5] Michael A Adams and Peter J Roughley. What is intervertebral disc degeneration, and what causes it? *SPINE*, 31:2151–2161, 2006.

[6] John Antoniou, Laura M. Epure, Arthur J. Michalek, Michael P. Grant, James C. Iatridis, and Fackson Mwale. Analysis of quantitative magnetic resonance imaging and biomechanical parameters on human discs with different grades of degeneration. *Journal of Magnetic Resonance Imaging*, 38:1402–1414, 12 2013.

[7] John Antoniou, Thomas Steffen, Fred Nelson, Neil Winterbottom, Anthony P. Hollander, Robin A. Poole, Max Aebi, and Mauro Alini. The human lumbar intervertebral disc: Evidence for changes in the biosynthesis and denaturation of the extracellular matrix with growth, maturation, ageing, and degeneration. *Journal of Clinical Investigation*, 98:996–1003, 8 1996.

[8] W C Bae, T Yoshikawa, R Znamirowski, A R Hemmad, B C Vande Berg, C B Chung, K Masuda, and G M Bydder. Ultrashort time-to-echo mri of human intervertebral disc endplate: Association with disc degeneration. *Proceedings of the International Society of Magnetic Resonance Imaging in Medicine*, 18, 2010.

[9] Lorin M. Benneker, Paul F. Heini, Suzanne E. Anderson, Mauro Alini, and Keita Ito. Correlation of radiographic and mri parameters to morphological and biochemical assessment of intervertebral disc degeneration. *European Spine Journal*, 14:27–35, 2 2005.

[10] B A Best and et al. Compressive mechanical properties of the human anulus fibrosus and their relationship to biochemical composition. *SPINE*, 1994.

[11] Semih E. Bezci, Aditya Nandy, and Grace D. O'Connell. Effect of hydration on healthy intervertebral disk mechanical stiffness. *Journal of Biomechanical Engineering*, 137, 10 2015.

[12] Scott D Boden. Abnormal magnetic-resonance scans of the cervical spine in asymptomatic subjects a prospective investigation*t. *THE JOURNAL OF BONE AND JOINT SURGERY*, 72A, 1990.

[13] Arijitt Borthakur, Philip M. Maurer, Matthew Fenty, Chenyang Wang, Rachelle Berger, Jonathon Yoder, Richard A. Balderston, and Dawn M. Elliott. T1 magnetic resonance imaging and discography pressure as novel biomarkers for disc degeneration and low back pain. *Spine*, 36:2190–2196, 12 2011.

[14] J J Cassidy, A Hiltner, and E Baer. Hierarchical structure of the intervertebral disc. 23:75–88, 1989.

[15] Deva D. Chan, Paull C. Gossett, Kent D. Butz, Eric A. Nauman, and Corey P. Neu. Comparison of intervertebral disc displacements measured under applied loading with mri at 3.0t and 9.4t. *Journal of Biomechanics*, 47:2801–2806, 8 2014.

[16] Deva D. Chan and Corey P. Neu. Intervertebral disc internal deformation measured by displacements under applied loading with mri at 3t. *Magnetic Resonance in Medicine*, 71:1231–1237, 2014.

[17] Elaine J Chiu, David C Newitt, Mark R Segal, Serena S Hu, Jeffrey C Lotz, and Sharmila Majumdar. Magnetic resonance imaging measurement of relaxation and water diffusion in the human lumbar intervertebral disc under compression in vitro. *SPINE*, 26:437–444, 2001.

[18] Tae Sub Chung, Young Jun Lee, Seong Woong Kang, Chang Jun Park, Won Suk Kang, and Yong Woon Shim. Reducibility of cervical disk herniation: Evaluation at mr imaging during cervical traction with a nonmagnetic traction device. *Radiology*, 225:895–900, 2002.

[19] Tae Sub Chung, Hea Eun Yang, Sung Jun Ahn, and Jung Hyun Park. Herniated lumbar disks: Realtime mr imaging evaluation during continuous traction. *Radiology*, 275:755–762, 6 2015.

[20] Nripendra Dhillon, Elisa C Bass, and Jeffrey C Lotz. Effect of frozen storage on the creep behavior of human intervertebral discs. *SPINE*, 26:883–888, 2001.

[21] Arin M. Ellingson, Tina M. Nagel, David W. Polly, Jutta Ellermann, and David J. Nuckley. Quantitative t2* (t2 star) relaxation times predict site specific proteoglycan content and residual mechanics of the intervertebral disc throughout degeneration. *Journal of Orthopaedic Research*, 32:1083–1089, 2014.

[22] James F Griffith, Yi-Xiang J Wang, Gregory E Antonio, Kai Chow Choi, Alfred Yu, Anil T Ahuja, and Ping Chung Leung. Modified pfirrmann grading system for lumbar intervertebral disc degeneration e708. *SPINE*, 32:708–712, 2007.

[23] Sarah E. Gullbrand, Beth G. Ashinsky, John T. Martin, Stephen Pickup, Lachlan J. Smith, Robert L. Mauck, and Harvey E. Smith. Correlations between quantitative t2 and t1 mri, mechanical properties and biochemical composition in a rabbit lumbar intervertebral disc degeneration model. *Journal of Orthopaedic Research*, 34:1382–1388, 8 2016.

[24] M. A. Hall-Craggs, J. Porter, P. D. Gatehouse, and G. M. Bydder. Ultrashort echo time (ute) mri of the spine in thalassaemia. *British Journal of Radiology*, 77:104–110, 2 2004.

[25] D Stephen Hickey and David W. L. Hukins. Relation between the structure of the annulus fibrosus and the function and failure of the intervertebral disc. *SPINE*, 5, 1980.

[26] W G Horton. Further observations on the elastic mechanism of the intervertebral disc*, 1958.

[27] M D Humzah and R W Soames. Human lntervertebral disc: Structure and function. *The Anatomical Record*, 220:337–356, 1988.

[28] James C. Iatridis, Steven B. Nicoll, Arthur J. Michalek, Benjamin A. Walter, and Michelle S. Gupta. Role of biomechanics in intervertebral disc degeneration and regenerative therapies: What needs repairing in the disc and what are promising biomaterials for its repair? *Spine Journal*, 13:243–262, 3 2013.

[29] James C. Iatridis, Mark Weidenbaum, Lori A. Setton, and Van C. Mow. Is the nucleus pulposus a solid or a fluid? mechanical behaviors of the nucleus pulposus of the human intervertebral disc. *SPINE*, 21:1174–1184, 1996.

[30] Wilke H. J., Wenger K., and Claes L. Testing criteria for spinal implants: recommendations for the standardization of in vitro stability testing of spinal implants. *SPINE*, 1998.

[31] J Janevic, J A Ashton-Miller, and A B Schultz. Large compressive preloads decrease lumbar motion segment flexibility. *Journal of Orthopaedic Research*, 9228, 1991.

[32] Wade Johannessen, Joshua D Auerbach, Andrew J Wheaton, Alykhan Kurji, Arijitt Borthakur, Ravinder Reddy, and Dawn M Elliott. Assessment of human disc degeneration and proteoglycan content using t 1-weighted magnetic resonance imaging. *SPINE*, 31:1253–1257, 2006.

[33] Wade Johannessen and Dawn M Elliott. Effects of degeneration on the biphasic material properties of human nucleus pulposus in confined compression. *SPINE*, 30:724–729, 2005.

[34] Thompson J.P., Pearce R. H., Schechter M. T., and Adams M. E. Preliminary evaluation of a scheme for grading the gross morphology of the human intervertebral disc. *SPINE*, 15, 1990.

[35] Noureddin Karimi, Parvin Akbarov, and Leila Rahnama. Effects of segmental traction therapy on lumbar disc herniation in patients with acute low back pain measured by magnetic resonance imaging: A single arm clinical trial. *Journal of Back and Musculoskeletal Rehabilitation*, 30:247–253, 2017.

[36] Girish Katti, Syeda Arshiya Ara, and Ayesha Shireen. Magnetic resonance imaging (mri)-a review. *INTERNATIONAL JOURNAL OF DENTAL CLINICS*, 3:65–70, 2011.

[37] Gang Un Kim, Min Cheol Chang, Tae Uk Kim, and Gun Woo Lee. Diagnostic modality in spine disease: A review. *Asian Spine Journal*,

14:910–920, 2020.

[38] B W Koes, M W Van Tulder, and S Thomas. Clinical review diagnosis and treatment of low back pain. *BMJ*, 332:1430–1434, 2006.

[39] Sang-Hun Lee, Scott D Daffner, and Jeffrey C Wang. Does lumbar disk degeneration increase segmental mobility in vivo? segmental motion analysis of the whole lumbar spine using kinetic mri. 2013.

[40] Matthias Philipp Lichy, Beate M Wietek, John P Mugler Iii, Wilhelm Horger, ¶ Marion, Irene Menzel, Aristotelis Anastasiadis, Katja Siegmann, Thomas Niemeyer, Arnulf Königsrainer, Berthold Kiefer, Fritz Schick, Claus D Claussen, and Heinz-Peter Schlemmer. Magnetic resonance imaging of the body trunk using a single-slab, 3-dimensional, t2-weighted turbo-spin-echo sequence with high sampling efficiency (space) for high spatial resolution imaging initial clinical experiences. *Investigative Radiology*, 40:754–760, 2005.

[41] Rose G. Long, Olivia M. Torre, Warren W. Hom, Dylan J. Assael, and James C. Iatridis. Design requirements for annulus fibrosus repair: Review of forces, displacements, and material properties of the intervertebral disk and a summary of candidate hydrogels for repair. *Journal of Biomechanical Engineering*, 138, 2 2016.

[42] Ghislain Maquer, Vaclav Brandejsky, Lorin M. Benneker, Atsuya Watanabe, Peter Vermathen, and Philippe K. Zysset. Human intervertebral disc stiffness correlates better with the otsu threshold computed from axial t2 map of its posterior annulus fibrosus than with clinical classifications. *Medical Engineering and Physics*, 36:219–225, 2 2014.

[43] N. L. Marinelli, Victor M. Haughton, and P. A. Anderson. T2 relaxation times correlated with stage of lumbar intervertebral disk degeneration and patient age. *American Journal of Neuroradiology*, 31:1278–1282, 8 2010.

[44] Marius E. Mayerhoefer, David Stelzeneder, Werner Bachbauer, Goetz H. Welsch, Tallal C. Mamisch, Piotr Szczypinski, Michael Weber, Nicky H.G.M. Peters, Julia Fruehwald-Pallamar, Stefan Puchner, and Siegfried Trattnig. Quantitative analysis of lumbar intervertebral disc abnormalities at 3.0 tesla: Value of t 2 texture features and geometric parameters. *NMR in Biomedicine*, 25:866–872, 6 2012.

[45] D W Mcmillan, G Garbutt, and M A Adams. Effect of sustained loading on the water content of intervertebral discs: implications for disc metabolism. *Ann Rheum Dis*, 55:880–887, 1996.

[46] D.S. McNally and M.A. Adams. Internal intervertebral disc mechanics as revealed by stress profilometry. *SPINE*, 17, 1992.

[47] W.D. Means. Kinematics, stress, deformation and material behavior. *Journal of Structural Geology*, pages 953–971, 1990.

[48] Rajiv G. Menon, Marcelo V.W. Zibetti, Martin Pendola, and Ravinder R. Regatte. Measurement of three-dimensional internal dynamic strains in the intervertebral disc of the lumbar spine with mechanical loading and golden-angle radial sparse parallel-magnetic resonance imaging. *Journal of Magnetic Resonance Imaging*, 54:486–496, 8 2021.

[49] Fackson Mwale, Caroline N. Demers, Arthur J. Michalek, Gilles Beaudoin, Tapas Goswami, Lorne Beckman, James C. Iatridis, and John Antoniou. Evaluation of quantitative magnetic resonance imaging, biochemical and mechanical properties of trypsin-treated intervertebral discs under physiological compression loading. *Journal of Magnetic Resonance Imaging*, 27:563–573, 3 2008.

[50] Fackson Mwale, James C. Iatridis, and John Antoniou. Quantitative mri as a diagnostic tool of intervertebral disc matrix composition and integrity. volume 17, 12 2008.

[51] Alf Nachemson. The influence of spinal movements on the lumbar intradiscal pressure and on the tensile stresses in the annulus fibrosus. *Acta Orthopaedica*, 33:183–207, 1963.

[52] Nandan L. Nerurkar, Dawn M. Elliott, and Robert L. Mauck. Mechanical design criteria for intervertebral disc tissue engineering. *Journal of Biomechanics*, 43:1017–1030, 4 2010.

[53] Nicolas Newell, Diagarajen Carpanen, Grigorios Grigoriadis, J. Paige Little, and Spyros D. Masouros. Material properties of human lumbar intervertebral discs across strain rates. *Spine Journal*, 19:2013–2024, 12 2019.

[54] Nicolas Newell, Grigorios Grigoriadis, Alexandros Christou, Diagarajen Carpanen, and Spyros D. Masouros. Material properties of bovine intervertebral discs across strain rates. *Journal of the Mechanical Behavior of Biomedical Materials*, 65:824–830, 1 2017.

[55] An M. Nguyen, Wade Johannessen, Jonathon H. Yoder, Andrew J. Wheaton, Edward J. Vresilovic, Arijitt Borthakur, and Dawn M. Elliott. Noninvasive quantification of human nucleus pulposus pressure with use of t1p-weighted magnetic resonance imaging. *Journal of Bone and Joint Surgery*, 90:796–802, 2008.

[56] G. Niu, Jian Yang, R. Wang, S. Dang, E. X. Wu, and Y. Guo. Mr imaging assessment of lumbar intervertebral disk degeneration and age-related changes: Apparent diffusion coefficient versus t2 quantitation. *American Journal of Neuroradiology*, 32:1617–1623, 10 2011.

[57] Grace D O'Connell, Wade Johannessen, Edward J Vresilovic, and Dawn M Elliott. Human internal disc strains in axial compression measured noninvasively using magnetic resonance imaging. *SPINE*, 32:2860–2868, 2007.

[58] Christian W A Pfirrmann, Alexander Metzdorf, Marco Zanetti, Juerg Hodler, and Norbert Boos. Magnetic resonance classification of lumbar intervertebral disc degeneration. *SPINE*, 26:1873–1878, 2001.

[59] D. Périé, J. C. Iatridis, C. N. Demers, T. Goswami, G. Beaudoin, F. Mwale, and J. Antoniou. Assessment of compressive modulus, hydraulic permeability and matrix content of trypsin-treated nucleus pulposus using quantitative mri. *Journal of Biomechanics*, 39:1392–1400, 2006.

[60] S Rajasekaran, J Naresh Babu, R Arun, B Roy, Wilson Armstrong, Ajoy Prasad Shetty, and Subramaniam Murugan. Issls prize winner: A study of diffusion in human lumbar discs: A serial magnetic resonance imaging study documenting the influence of the endplate on diffusion in normal and degenerate discs. *SPINE*, 29:2654–2667, 2004.

[61] Maximilien Recuerda, Delphine Périé, Guillaume Gilbert, and Gilles Beaudoin. Assessment of mechanical properties of isolated bovine intervertebral discs from multi-parametric magnetic resonance imaging. *BMC Musculoskeletal Disorders*, 13, 2012.

[62] David A. Reiter, Fadi A. Fathallah, Rida T. Farouki, and Jeffery H. Walton. Noninvasive high resolution mechanical strain maps of the spine intervertebral disc using nonrigid registration of magnetic resonance images. *Journal of Biomechanics*, 45:1534–1539, 5 2012.

[63] Dae Cheol Rim. Quantitative pfirrmann disc degeneration grading system to overcome the limitation of pfirrmann disc degeneration grade. *Korean Journal of Spine*, 13:1, 2016.

[64] Neil Roberts, Christophe Gratin, and Graham H. Whitehouse. Mri analysis of lumbar intervertebral disc height in young and older populations. *Journal of Magnetic Resonance Imaging*, 7:880–886, 9 1997.

[65] Peter J Roughley. Biology of intervertebral disc aging and degeneration involvement of the extracellular matrix. *SPINE*, 29:2691–2699, 2004.

[66] A. Saifuddin, S. Blease, and E. Macsweeney. Axial loaded mri of the lumbar spine. *Clinical Radiology*, 58:661–671, 9 2003.

[67] Y. Schroeder, D. M. Elliott, W. Wilson, F. P.T. Baaijens, and J. M. Huyghe. Experimental and model determination of human intervertebral disc osmoviscoelasticity. *Journal of Orthopaedic Research*, 26:1141–1146, 8 2008.

[68] Zhi Shan, Shengyun Li, Junhui Liu, Maiwulanjiang Mamuti, Chongyan Wang, and Fengdong Zhao. Correlation between biomechanical properties of the annulus fibrosus and magnetic resonance imaging (mri) findings. *European Spine Journal*, 24:1909–1916, 9 2015.

[69] Si Shen, Hao Wang, Jing Zhang, Fei Wang, and Si Run Liu. Diffusion weighted imaging, diffusion tensor imaging, and t2* mapping of lumbar intervertebral disc in young healthy adults. *Iranian Journal of Radiology*, 13:1–9, 1 2016.

[70] Marc A. Stadelmann, Ghislain Maquer, Benjamin Voumard, Aaron Grant, David B. Hackney, Peter Vermathen, Ron N. Alkalay, and Philippe K. Zysset. Integrating mri-based geometry, composition and

fiber architecture in a finite element model of the human intervertebral disc. *Journal of the Mechanical Behavior of Biomedical Materials*, 85:37–42, 9 2018.

[71] S. Tavana, J. N. Clark, J. Prior, N. Baxan, S. D. Masouros, N. Newell, and U. Hansen. Quantifying deformations and strains in human intervertebral discs using digital volume correlation combined with mri (dvc-mri). *Journal of Biomechanics*, 102, 3 2020.

[72] S. Tavana, B. Davis, I. Canali, K. Scott, J.J.H. Leong, B.A. Freedman, and N. Newell. A novel tool to quantify in vivo lumbar spine kinematics and 3d intervertebral disc strains using clinical mri. *Journal of the Mechanical Behavior of Biomedical Materials*, 140, 4 2023.

[73] Zeliha Unlu, Saliha Tasci, Serdar Tarhan, Yuksel Pabuscu, and Serap Islak. Comparison of 3 physical therapy modalities for acute pain in lumbar disc herniation measured by clinical evaluation and magnetic resonance imaging. *Journal of Manipulative and Physiological Therapeutics*, 31:191–198, 3 2008.

[74] Jill P.G. Urban and C. Peter Winlove. Pathophysiology of the intervertebral disc and the challeges for mri. *Journal of Magnetic Resonance Imaging*, 25:419–432, 2 2007.

[75] Stefania Vaga, Manuela Teresa Raimondi, Enrico Gianluca Caiani, Francesco Costa, Carmen Giordano, Franco Perona, Alberto Zerbi, and Maurizio Fornari. Quantitative assessment of intervertebral disc glycosaminoglycan distribution by gadolinium-enhanced mri in orthopedic patients. *Magnetic Resonance in Medicine*, 59:85–95, 2008.

[76] Chenyang Wang, Walter Witschey, Mark A. Elliott, Arijitt Borthakur, and Ravinder Reddy. Measurement of intervertebral disc pressure with t1 mri. *Magnetic Resonance in Medicine*, 64:1721–1727, 2010.

[77] Atsuya Watanabe, Lorin M. Benneker, Chris Boesch, Tomoko Watanabe, Takayuki Obata, and Suzanne E. Anderson. Classification of intervertebral disk degeneration with axial t2 mapping. *American Journal of Roentgenology*, 189:936–942, 10 2007.

[78] Dominik Weishaupt and Larissa Boxheimer. Dynamic and functional musculoskeletal imaging, 2003.

[79] Goetz Hannes Welsch, Siegfried Trattnig, Tatjana Paternostro-Sluga, Klaus Bohndorf, Sabine Goed, David Stelzeneder, and Tallal Charles Mamisch. Parametric t2 and t2* mapping techniques to visualize intervertebral disc degeneration in patients with low back pain: Initial results on the clinical use of 3.0 tesla mri. *Skeletal Radiology*, 40:543–551, 5 2011.

[80] Jan Willén and Barbro Danielson. The diagnostic effect from axial loading of the lumbar spine during computed tomography and magnetic resonance imaging in patients with degenerative disorders. *SPINE*, 26:2607–2614, 2001.

[81] Bo Yang, Michael F. Wendland, and Grace D. O'Connell. Direct quantification of intervertebral disc water content using mri. *Journal of Magnetic Resonance Imaging*, 52:1152–1162, 10 2020.

[82] Jonathon H. Yoder, John M. Peloquin, Gang Song, Nick J. Tustison, Sung M. Moon, Alexander C. Wright, Edward J. Vresilovic, James C. Gee, and Dawn M. Elliott. Internal three-dimensional strains in human intervertebral discs under axial compression quantified noninvasively by magnetic resonance imaging and image registration. *Journal of Biomechanical Engineering*, 136, 11 2014.

[83] Shiwei Yu, Victor M Haughton, Kenneth L Lynch, Khang-Cheng Ho, and Lowell A Sether. Fibrous structure in the intervertebral disk: Correlation of mr appearance with anatomic sections. *AJNR*, 10:1105–1110, 1989.

[84] Wei Zhang, Xiaohui Ma, Yan Wang, Jian Zhao, Xujing Zhang, Yu Gao, and Shiling Li. Assessment of apparent diffusion coefficient in lumbar intervertebral disc degeneration. *European spine journal : official publication of the European Spine Society, the European Spinal Deformity Society, and the European Section of the Cervical Spine Research Society*, 23:1830–1836, 9 2014.

[85] Bruno Beomonte Zobel, Gianluca Vadalà, Riccardo Del Vescovo, Sofia Battisti, Francesca Maria Martina, Luigi Stellato, Emanuele Leoncini, Arijitt Borthakur, and Vincenzo Denaro. T1 magnetic resonance imaging quantification of early lumbar intervertebral disc degeneration in healthy young adults. *Spine*, 37:1224–1230, 1 2012.

[86] Jin Zuo, Gabby B. Joseph, Xiaojuan Li, Thomas M. Link, Serena S. Hu, Sigurd H. Berven, John Kurhanewitz, and Sharmila Majumdar. In vivo intervertebral disc characterization using magnetic resonance spectroscopy and t 1 imaging: Association with discography and oswestry disability index and short form-36 health survey. *Spine*, 37:214–221, 2 2012.